Bimodality and hysteresis in systems driven by confined Lévy flights

Bartłomiej Dybiec and Ewa Gudowska-Nowak[1]

The Marian Smoluchowski Institute of Physics and Mark Kac Center for Complex Systems Research, Jagellonian University, ul. Reymonta 4, 30–059 Kraków, Poland
E-mail: bartek@th.if.uj.edu.pl and gudowska@th.if.uj.edu.pl

Abstract. We demonstrate the occurrence of bimodality and dynamical hysteresis in a system describing an overdamped quartic oscillator perturbed by additive white and asymmetric Lévy noise. Investigated estimators of the stationary probability density profiles display not only a turnover from unimodal to bimodal character but also a change in a relative stability of stationary states that depends on the asymmetry parameter of the underlying noise term. When varying the asymmetry parameter cyclically, the system exhibits a hysteresis in the occupation of a chosen stationary state.

Contents

[1] Author to whom any correspondence should be addressed.

1. Introduction

The Langevin description of an overdamped Brownian motion in a potential $V(x)$

$$\dot{x}(t) = -V'(x) + \zeta(t), \tag{1}$$

constitutes a basic paradigm to study the effects of fluctuations at the mesoscopic scale [1]–[3]. Here, prime stands for differentiation over x, and $\zeta(t)$ is a commonly assumed white Gaussian noise representing close-to-equilibrium fluctuations of the dynamic variable x. In contrast, in far-from-equilibrium situations, the Gaussianity of the noise term may be questionable, due to e.g. strong interaction with the surrounding 'bath' [4, 5]. Natural generalizations to the Brownian motion are then δ-correlated Lévy stable processes which can be interpreted as fluctuations resulting from strong collisions between the test particle and the environment. In particular, the scale-free, self similar feature of Lévy distributions gives rise to the occurrences of large increments of the position coordinates Δx during small time intervals causing a non-local character of the motion. Within the paper, we address the problem of kinetics as described by equation (1) under the action of $\zeta(t)$ representing a stationary white Lévy noise [6, 7]. Accordingly, the position of the Brownian particle subjected to additive white Lévy noise is calculated by direct integration of equation (1) with respect to the α-stable measure [6]–[11] $L_{\alpha,\beta}(s)$, i.e. $x(t + \Delta t) = x(t) - V'(x(t))\Delta t + (\Delta t)^{1/\alpha}\zeta$, where ζ is distributed according to the α-stable Lévy type distribution $L_{\alpha,\beta}(\zeta; \sigma, \mu = 0)$ whose representation [6, 8] is given by the characteristic function $\phi(k)$ defined in the Fourier space $\phi(k) = \mathcal{F}(L_{\alpha,\beta}(\zeta; \sigma, \mu)) = \int_{-\infty}^{\infty} d\zeta\, e^{ik\zeta} L_{\alpha,\beta}(\zeta; \sigma, \mu)$

$$\phi(k) = \exp\left[-\sigma^{\alpha}|k|^{\alpha}\left(1 - i\beta\,\mathrm{sgn}(k)\tan\frac{\pi\alpha}{2}\right) + i\mu k\right], \quad \text{for } \alpha \neq 1 \tag{2}$$

$$\phi(k) = \exp\left[-\sigma|k|\left(1 + i\beta\frac{2}{\pi}\mathrm{sgn}(k)\ln|k|\right) + i\mu k\right], \quad \text{for } \alpha = 1. \tag{3}$$

The stability index α, determining tails of the probability density function (PDF) takes values $\alpha \in (0, 2]$, the skewness of the distribution is modeled by the asymmetry parameter $\beta \in [-1, 1]$. Indices α and β classify the type of stable distributions up to translations and dilations [6, 8]. Two other parameters of scaling $\sigma \in (0, \infty)$ and location $\mu \in (-\infty, \infty)$ can vary, although replacing $\zeta - \mu$ and $\sigma\zeta$ in the original coordinates shifts the origin and rescales the abscissa without altering the function $L_{\alpha,\beta}(\zeta)$. For simplicity, we will restrict ourselves here to strictly stable Lévy noise with $\mu = 0$ [6, 8]. Generally, for $\beta = \mu = 0$ PDFs are symmetric while for $\beta = \pm 1$ and $\alpha \in (0, 1)$ they are totally skewed, i.e. ζ is always positive or negative only, depending on the sign of the asymmetry parameter β (cf figure 1). Asymptotically, for $\zeta \to \infty$ with $\alpha < 2$, stable PDFs behave as $p(\zeta) \propto |\zeta|^{-(\alpha+1)}$ causing divergence of moments $\langle \zeta^{\nu} \rangle = \infty$ for $\nu < \alpha$. The asymmetry is reflected in a biased distribution $\lim_{\zeta \to \infty} \frac{\mathrm{prob}(Z > \zeta)}{\mathrm{prob}(|Z| > \zeta)} = \frac{1+\beta}{2}$.

For $\alpha \neq 1$, equivalent to the stochastic ordinary differential equation (1) is a fractional Fokker–Planck equation (FFPE) [12]–[17] for the probability distribution function

$$\frac{\partial p(x,t)}{\partial t} = \frac{\partial}{\partial t}\int_{-\infty}^{\infty}\frac{dk}{2\pi}\phi(k,t)e^{-ikx}$$

$$= \int_{-\infty}^{\infty}\frac{dk}{2\pi}\phi(k,t)e^{-ikx}\left[i\mu k - \sigma^{\alpha}|k|^{\alpha} + i\beta\sigma^{\alpha}k|k|^{\alpha-1}\tan\frac{\pi\alpha}{2}\right]$$

$$= -\sigma^{\alpha}(-\Delta)^{\alpha/2}p(x,t) - \sigma^{\alpha}\beta\tan\frac{\pi\alpha}{2}\frac{\partial}{\partial x}(-\Delta)^{(\alpha-1)/2}p(x,t) - \mu\frac{\partial}{\partial x}p(x,t), \tag{4}$$
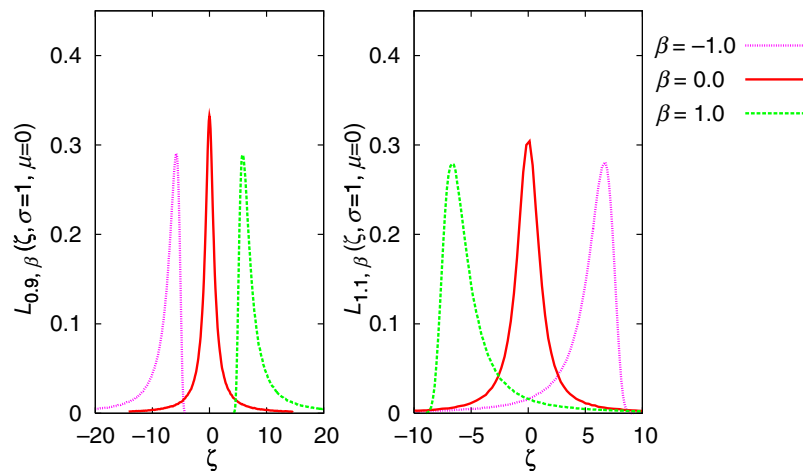
Figure 1. Sample α-stable PDFs with $\alpha = 0.9$ (left panel) and $\alpha = 1.1$ (right panel). For $\beta = 0$ distributions are symmetric and become asymmetric for $\beta \neq 0$. The support of the densities for the fully asymmetric cases with $\beta = \pm 1$ and $\alpha < 1$ (left panel) assumes only negative values for $\beta = -1$ and only positive values for $\beta = 1$. Note the differences in the positions of the maxima for $\alpha < 1$ and $\alpha > 1$.

with $p(x, t)$ representing the PDFs for finding a particle at time t in the vicinity of x, $\phi(k, t) = \langle \exp[ikx(t)] \rangle = \langle \exp[ik \int_0^t \zeta(s)\mathrm{d}s] \rangle$ standing for the characteristic function of the stable process and $-\Delta^\alpha f(x)$ denoting the fractional Laplacian [18] $-(\Delta)^{\alpha/2} f(x) = \mathcal{F}^{-1}(|k|^\alpha \hat{f}(k))$, with $\alpha = 2$ corresponding to the standard Brownian diffusion case. The addition of the potential force $-V'(x)$ to equation (1) adds the classical drift term $\frac{\partial}{\partial x}[V'(x)p(x, t)]$ to equation (4). In the approach presented herein, instead of solving equation (4), information on the system is drawn from the statistics of numerically [6, 8] generated trajectories satisfying the generalized Langevin equation (1). At a single trajectory level sampled from the stochastic dynamic study of the problem, the initial condition for equation (1) has been set to $x(0) \stackrel{\mathrm{d}}{=} \mathcal{U}[-1, 1]$, i.e. the initial position of the particle is drawn from the uniform distribution over the interval $[-1, 1]$. For simplicity, equation (1) has been studied in dimensionless variables [19, 20] with additionally setting $\sigma = 1$. The time independent potential $V(x)$ is assumed to be of the form $V(x) = x^4/4$ which guarantees the confinement of the trajectory $x(t)$ within the potential well [19, 21, 22] leading to a finite variance of the stationary PDF. For general α-stable driving and a quartic potential the stationary PDF fulfils

$$\frac{\partial^3 \hat{P}(k)}{\partial k^3} = \mathrm{sgn}k|k|^{\alpha-1}\hat{P}(k) - \mathrm{i}\beta \tan\frac{\pi\alpha}{2}|k|^{\alpha-1}\hat{P}(k), \tag{5}$$

where $\hat{P}(k)$ stands for a Fourier transform of the stationary PDF, $P(x) = \lim_{t\to\infty} p(x, t)$. Analytical solutions of equation (5) can be readily obtained for a Gaussian case ($\alpha = 2$, arbitrary β): $P(x) = \Gamma(3/4)\exp(-x^4/4)/\pi$ and for Cauchy additive noise ($\alpha = 1$, $\beta = 0$): $P(x) = 1/[\pi(1 - x^2 + x^4)]$ [19, 21, 22]. They display a perfect agreement (cf figure 2) with profiles of PDFs obtained by numerical simulations of equation (1) performed with the Janicki–Weron algorithm [6, 8, 23, 24].
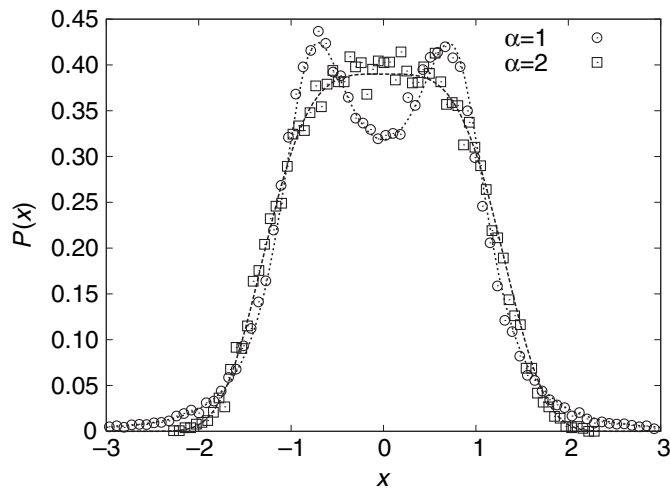
Figure 2. Stationary PDFs for $\alpha = 2$ (Gaussian case, unimodal distribution) and $\alpha = 1.0$ (Cauchy case, bimodal distribution) with corresponding analytical solutions. Numerical results were constructed for $\Delta t = 10^{-4}$, $T_{max} = 10$ and averaged over $N = 5 \times 10^4$ realizations.

2. Results

Numerical results were constructed for a time step of integration $\Delta t = 10^{-4}$, simulation length $T_{max} = 10$ with an overall statistics of $N = 5 \times 10^4$ realizations. To check whether results are influenced by the length of simulations, results for various T_{max} ($T_{max} = 10$ and 15) were compared showing consistency of estimated PDFs for both values. Further details on values of parameters are included in the text accompanying the figures. Numerical examination of equation (1) allows for construction of PDF estimators for the whole range of parameters α and β. Likewise, by direct integration of equation (1) it is also possible to investigate time-dependent PDFs and noise-induced bimodality of the probability distribution [19, 21, 22, 25, 26]. Note that this approach, if applied for noise sources represented by the generalized Lévy–Gnedenko central limit theorem, would lead to stationary distributions which are not of the usual Boltzmann–Gibbs type [27, 28].

The change of α (for $\beta \neq 0$) from values >1 to values <1 results in a change of location of a modal value of stable densities, see left versus right panel of figure 1. The shift of modal values is reflected in properties of stationary states. For $\alpha > 1$ with $\beta < 0$ the modal value is located for $x > 0$ (right panel of figure 3) while for $\alpha < 1$ with $\beta < 0$ it shifts to the negative interval $x < 0$ (left panel of figure 3). For $\beta < 0$ modal values are located on the opposite side of the origin than for $\beta > 0$. Therefore, the position of the modal value can be moved from the positive to negative real lines by change of α while β is kept constant (left versus right panel of figure 3) or by change of β to $-\beta$ with a preset value of α (cf different rows in figure 3).

The fact that changes in β can change the location of the modal value suggests that periodic changes in this parameter can lead to a phenomenon resembling dynamical hysteresis [29]–[31]. In order to register a hysteretic behavior of the system, we have performed an analysis of trajectories of equation (1) based on a two-state approximation. For this purpose, we have
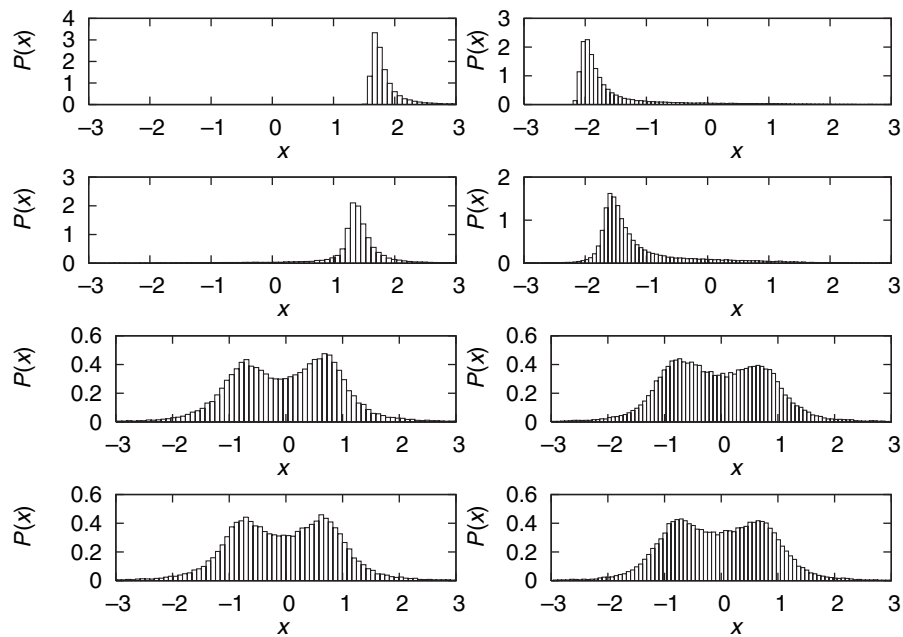
Figure 3. Stationary probability distributions $P(x)$ for $\alpha = 0.9$ (left column) and $\alpha = 1.1$ (right column). Various rows correspond to the various values of β, starting from the top panel: $\beta = 1$ (top row), $\beta = 0.5, 0.01$ and $\beta = 0$ (bottom row). Due to symmetry, results for negative β can be obtained by the reflection of results for $\beta \geqslant 0$ along the $x = 0$ line. Results were constructed for $\Delta t = 10^{-4}$, $T_{\max} = 10$ and averaged over $N = 5 \times 10^4$ realizations.

defined an occupation probability of being in left/right state according to

$$p_t(\text{left}) = \text{prob}\{x(t) < 0\} = \int_{-\infty}^{0} p(x, t)\mathrm{d}x = 1 - p_t(\text{right}). \quad (6)$$

Transition between the states is induced by the time dependent asymmetry parameter β which is periodically modulated over time, i.e. $\beta = \beta_{\max} \sin \Omega t = \beta_{\max} \sin \frac{2\pi}{T_\Omega} t$. In figure 4, values of $p(\text{left})$ for various T_Ω (with $\beta_{\max} = 1$) are presented. Stable random variables for $\alpha < 1$ with $|\beta| = 1$ take only positive/negative values, depending on the sign of β. Therefore a higher level of saturation is observed for $\alpha = 0.9$ (left panel) than for $\alpha = 1.1$ (right panel), i.e., when $|\beta| = 1$ the probability of being in the left/right state for $\alpha = 0.9$ (left panel) is higher than for $\alpha = 1.1$ (right panel). The direction of the hysteresis loop is a direct consequence of the fact that changes in β move modal values from the positive/negative real line to the negative/positive real line. Due to the initial condition imposed on $x(0)$, the starting point for each hysteresis loop is (0,0.5) and the first part of the curve describes approaching to the proper hysteresis loop. With decreasing Ω (increasing T_Ω) the area of the hysteresis loop decreases because the system has more time for relaxation and response to the changes of β. For large Ω (small T_Ω) the response of the system is more delayed and consequently the area of the hysteresis loop is larger.

Finally the influence of $\beta_{\max}$ on the shape of the hysteresis loop has been examined. In figure 5, hysteresis loops for various $\beta_{\max}$ (with $T_\Omega = 9$) are presented. Smaller $\beta_{\max}$ makes
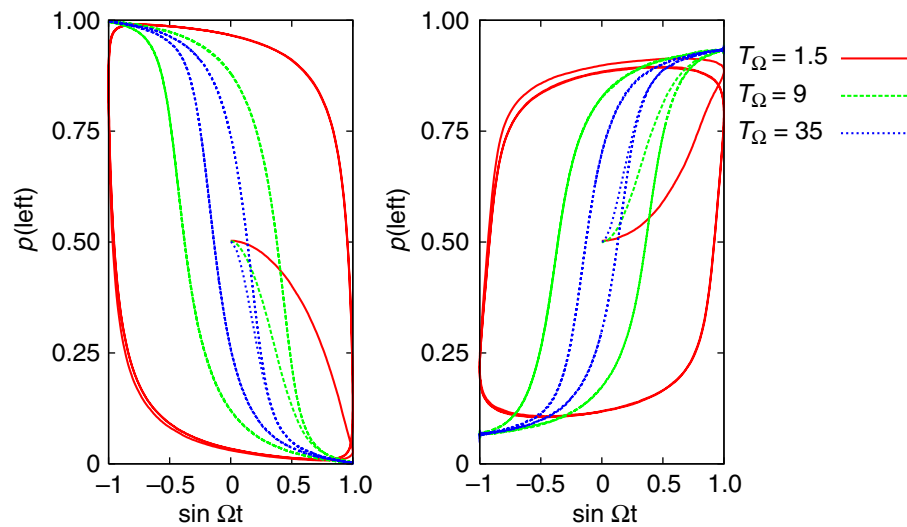
Figure 4. Hysteresis loops for $\alpha = 0.9$ (left panel) and $\alpha = 1.1$ (right panel). Different lines correspond to the different values of T_{Ω}, amplitude of β $\beta_{max} = 1.0$. Results were constructed for $\Delta t = 10^{-3}$ and averaged over $N = 10^5$ realizations. Various loops correspond to different values of the driving period T_{Ω}: $T_{\Omega} = 35$, 9, and 1.5 (from inside to outside).
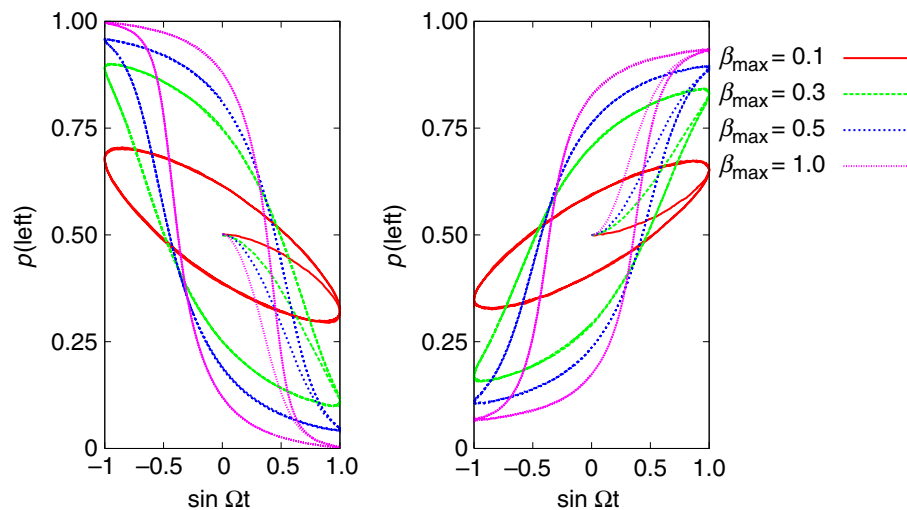

Figure 5. Hysteresis loops for $\alpha = 0.9$ (left panel) and $\alpha = 1.1$ (right panel). Different lines correspond to the different values of β_{max}, driving period $T_{\Omega} = 9$. Results were constructed for $\Delta t = 10^{-3}$ and averaged over $N = 10^5$ realizations. Various loops correspond to different values of β_{max}: $\beta_{max} = 1.0$, 0.5, 0.3 and 0.1 (from top to bottom).

stable distribution less skewed and as a consequence, less probability mass becomes located in the left state and the effect of saturation is less visible. Furthermore, with decreasing β_{max}, loops become more oval and finally for $\beta_{max} = 0$ the hysteresis phenomenon disappears.

3. Summary and conclusions

A standard approach to equation (1) assumes a Gaussian character of the noise term describing interaction of the studied system with its complex surroundings. An additional assumption about the existence of timescale separation between the dynamics of the observable $x(t)$ and the typical timescale of the noise allows external fluctuations to be modeled as temporally uncorrelated and therefore 'white.' However, in many natural phenomena the assumptions concerning properties of 'gaussianity' and 'whiteness' of the noise can be violated [5, 32]. In this context, in contrast to the spatiotemporal coupling characterizing general forms of non-Markovian or semi-Markovian Lévy walks, Lévy flights correspond to the class of Markov processes which still can be interpreted as white, but distributed according to a more general, infinitely divisible, stable and non-Gaussian law [6, 8].

Lévy noise-driven non-equilibrium systems are known to manifest interesting physical properties and have been addressed in various realms, ranging from the description of the dynamics in plasmas, diffusion in energy space, self-diffusion in micelle systems, exciton and charge transport in polymers under conformational motion and incoherent atomic radiation trapping [5, 33, 34] to the spectral analysis of paleoclimatic [35, 36] or economic data [37], motion in optimal search strategies among randomly distributed target sites, fluorophore diffusion as studied in photobleaching experiments [38] and many others.

As discussed in this paper, the modulation of stable noise parameters modifies the shape of the stationary probability density corresponding to the Langevin equation (1). In particular, skewed noise characterized by the non-zero asymmetry parameter β can induce asymmetry of stationary states in symmetric potentials. Furthermore, totally skewed stable noise ($\alpha < 1$ with $|\beta| = 1$) could move the probability mass to one side of the x-axis making stationary states totally skewed. In such situations, the whole probability mass can be located on the left-hand side or on the right-hand side of the origin $x = 0$ depending on the sign of the asymmetry parameter β. For $\alpha > 1$ with a non-zero β, the stable noise is still asymmetric. Nevertheless, even $|\beta| = 1$ is not sufficient to induce totally skewed stationary states. Consequently, dynamical hysteresis loops induced by cyclic variation of β for $\alpha < 1$ and $\alpha > 1$ are characterized by various levels of saturation, see left versus right panel of figure 4.

The model system presented in this study assumes action of the monostable quartic potential which leads to the confinement of $x(t)$ trajectories and bounded stationary states, i.e. states with finite variance. Nevertheless, the similar hysteretic behavior can be also observed in a harmonic potential. In this case, however, the stationary probability density assumes a Lévy stable form with the same stability, α, and asymmetry, β, indices as the underlying noise. In consequence, modulation of the asymmetry parameter β results in shifts of the location of the PDF-modal value causing different fractions of the probability mass to be located to the left or to the right of the origin $x = 0$. Moreover, in contrast to the quartic potential, the action of the parabolic one does not confine the Lévy-flight trajectories causing much larger fluctuations of a particle position with diverging variance.

Another method to present the results for stationary distributions (cf figure 3) is the use of the effective potential [20]. In general, at a given time point t the same probability densities

IOP Institute of Physics **Φ** DEUTSCHE PHYSIKALISCHE GESELLSCHAFT

that are recorded for the system under the action of the quartic potential and α stable noise can be observed in the Gaussian regime with the effective potential $V_{\text{eff}}(x, t) = -\log[p(x, t)]$. Despite the fact that the one-point probability densities for the system $\dot{x}(t) = -V'_{\text{eff}}(x, t) + \xi(t)$ with white and Gaussian noise $\xi(t)$ ($\langle\xi(t)\xi(t')\rangle = \delta(t - t')$) are the same, other characteristics of these two processes remain distinctly different.

Also construction of the dynamical hysteresis for the effective model is more complicated than just examination of equation (1) with $V_{\text{eff}}(x, t)$. Parametric time-dependence of the effective potential (via time-dependence of β) and lack of general analytical solutions for $p(x, t)$, both require $V_{\text{eff}}(x, t)$ to be determined numerically. Moreover, such an approach is much more computationally demanding because it needs the effective potential to be numerically constructed at all $T_\Omega/\Delta t$ points.

The dynamical hysteresis can be also observed in the generic double well potential model subject to the joint action of the deterministic periodic modulation and stochastic α-stable fluctuations [39]. In such a case, however, the shape of the dynamical hysteresis loop is affected both by the character of the noise and by the type of periodic modulation [30, 39].

Altogether, the dynamical hysteresis detected in the model described by equation (1) emerges as a consequence of periodical modulation of the asymmetry parameter β. In the effective potential model, periodical modulation of the asymmetry parameter corresponds to the periodical modulation of the effective potential $V_{\text{eff}}(x, t)$. Nevertheless, as argued above, the two models are not fully equivalent pointing out that a mere examination of one-point probability densities is not a sufficiently conclusive method for discrimination of underlying types of noise.

Acknowledgments

References

[1] van Kampen N G 1981 *Stochastic Processes in Physics and Chemistry* (Amsterdam: North-Holland)
[2] Gammaitoni L, Hänggi P, Jung P and Marchesoni F 1998 Stochastic resonance *Rev. Mod. Phys.* **70** 223
[3] Anishchenko V S, Neiman A B, Moss F and Schimansky-Geier L 1992 Stochastic resonance: noise-enhanced order *Phys.—Usp.* **42** 7
[4] Klimontovich Y L 1994 *Statistical Physics of Open Systems* (Dordrecht: Kluwer)
[5] Shlesinger M F, Zaslavsky G M and Frisch J (ed) 1995 *Lévy Flights and Related Topics in Physics* (Berlin: Springer)
[6] Janicki A and Weron A 1994 *Simulation and Chaotic Behavior of α-Stable Stochastic Processes* (New York: Marcel Dekker)
[7] Dybiec B, Gudowska-Nowak E and Hänggi P 2007 Escape driven by α-stable white noises *Phys. Rev.* E **75** 021109
[8] Janicki A 1996 *Numerical and Statistical Approximation of Stochastic Differential Equations with Non-Gaussian Measures* (Wrocław: Hugo Steinhaus Centre for Stochastic Methods)
[9] Dybiec B and Gudowska-Nowak E 2004 Resonant activation in the presence of nonequilibrated baths *Phys. Rev.* E **69** 016105

[10] Dybiec B and Gudowska-Nowak E 2004 Resonant activation driven by strongly non-Gaussian noises *Fluct. Noise Lett.* **4** L273

[11] Dybiec B, Gudowska-Nowak E and Hänggi P 2006 Lévy-Brownian motion on finite intervals: mean first passage time analysis *Phys. Rev.* E **73** 046104

[12] Fogedby H C 1998 Lévy flights in quenched random force fields *Phys. Rev.* E **58** 1690

[13] Metzler R, Barkai E and Klafter J 1999 Deriving fractional Fokker–Planck equations from a generalized master equation *Europhys. Lett.* **46** 431

[14] Yanovsky V V, Chechkin A V, Schertzer D and Tur A V 2000 Lévy anomalous diffusion and fractional Fokker–Planck equation *Physica* A **282** 13

[15] Schertzer D, Larchevêque M, Duan J, Yanowsky V V and Lovejoy S 2001 Fractional Fokker–Planck equation for nonlinear stochastic differential equations driven by non-Gaussian Lévy stable noises *J. Math. Phys.* **42** 200

[16] Dubkov A A and Spagnolo B 2005 Generalized Wiener process and Kolmogorov's equation for diffusion induced by non-Gaussian noise source *Fluct. Noise Lett.* **5** L267

[17] Dubkov A A and Spagnolo B 2007 Langevin approach to Lévy flights in fixed potentials: exact results for stationary probability distributions *Acta Phys. Pol.* B **38** 1745

[18] Jespersen S, Metzler R and Fogedby H C 1999 Lévy flights in external force fields: Langevin and fractional Fokker–Planck equations and their solutions *Phys. Rev.* E **59** 2736

[19] Chechkin A V, Klafter J, Gonchar V Y, Metzler R and Tanatarov L V 2002 Stationary states of non-linear oscillators driven by Lévy noise *Chem. Phys.* **284** 233

[20] Dybiec B, Gudowska-Nowak E and Sokolov I M 2007 Stationary states in Langevin dynamics under asymmetric Lévy noises *Phys. Rev.* E **76** 041122

[21] Chechkin A V, Klafter J, Gonchar V Y, Metzler R and Tanatarov L V 2003 Bifurcation, bimodality and finite variance in confined Lévy flights *Phys. Rev.* E **67** 010102

[22] Chechkin A V, Gonchar V Y, Klafter J, Metzler R and Tanatarov L V 2004 Lévy flights in a steep potential well *J. Stat. Phys.* **115** 1505

[23] Weron A and Weron R 1995 Computer simulation of Lévy stable variables and processes *Lecture Notes Phys.* **457** 379

[24] Weron R 1996 On the Chambers–Mallows–Stuck method for simulating skewed stable random variables *Stat. Probab. Lett.* **28** 165

[25] Mierzejewski M, Dajka J, Luczka J, Talkner P and Hänggi P 2006 Dynamical bimodality in equilibrium monostable systems *Phys. Rev.* E **74** 041102

[26] Dybiec B and Schimansky-Geier L 2007 Emergence of bimodality in noisy systems with single-well potential *Eur. Phys. J.* B **57** 313

[27] Barkai E 2003 Stable equilibrium based on Lévy statistics: stochastic collision models approach *Phys. Rev.* E **68** 055104

[28] Barkai E 2004 Stable equilibrium based on Lévy statistics: a linear Boltzmann equation approach *J. Stat. Phys.* **115** 1572

[29] Gudowska-Nowak E, Dybiec B and Flyvbjerg H 2004 Resonant effects in voltage activated channel gating *Proc. SPIE* **5467** 223

[30] Juraszek J, Dybiec B and Gudowska-Nowak E 2005 Hysteresis and synchronization in a two-level system driven by external noise *Fluct. Noise Lett.* **5** L259

[31] Pustovoit M A, Berezhkovskii A M and Bezrukov S M 2006 Analytical theory of hysteresis in ion channels: two-state model *J. Chem. Phys.* **125** 194907

[32] Brockmann D and Sokolov I M 2002 Lévy flights in external force fields: from models to equations *Chem. Phys.* **284** 409

[33] Sokolov I M, Mai J and Blumen A 1997 Paradoxal diffusion in chemical space for nearest-neighbor walks over polymer chains *Phys. Rev. Lett.* **79** 857

[34] Pereira E, Martinho J M G and Berberan-Santos M N 2004 Photon trajectories in incoherent radiation trapping as Lévy flights *Phys. Rev. Lett.* **93** 120201

[35] Ditlevsen P D 1999 Observation of α-stable noise induced millennial climate changes from an ice core record *Geophys. Res. Lett.* **26** 1441

[36] Ditlevsen P D, Kristensen M S and Andersen K K 2005 The recurrence time of Dansgaard–Oeschger events and limits on the possible periodic component *J. Clim.* **18** 2594

[37] Santini P 2000 Lévy scaling in random walks with fluctuating variance *Phys. Rev.* E **61** 93

[38] Periasamy N and Verkman A S 1998 Analysis of fluorophore diffusion by continuous distributions of diffusion coefficients: application to photobleaching measurements of multicomponent and anomalous diffusion *Biophys. J.* **75** 557

[39] Dybiec B and Gudowska-Nowak E 2007 Quantifying noise induced effects in the generic double-well potential *Acta Phys. Pol.* B **38** 1759